J. Astrophys. Astr. (1987) **8,** 343–350

An Analytical Approximation of the Hubble Space Telescope Monochromatic Point Spread Functions

O. Bendinelli *Dipartimento di Astronomia, Università di Bologna, Via Zamboni 33, 40126 Bologna, Italy*

G. Parmeggiani *Osservatorio Astronomico di Bologna, Via Zamboni 33, 40126 Bologna, Italy*

F. Zavatti *Dipartimento di Astronomia, Università di Bologna, Via Zamboni 33, 40126 Bologna, Italy*

Received 1987 June 16; accepted 1987 October 7

Abstract. A mixture of off-centred Gaussians is used to approximate the predicted monochromatic point spread functions (PSFs) of Hubble space telescope (HST) at long wavelengths, and also, with a reduced number of parameters, the wide-band PSFs. The usefulness of the approximation in simulation and analysis of HST data is shown by means of application to image centring and convolution-deconvolution problems.

Key words: HST, point spread function—image centring—image deconvolution

1, Introduction

The basic information on the expected image quality of the Hubble space telescope (HST) is reported in the last Announcement of Opportunity (NASA 1984, A.O.No.OSSA-4-84, hereinafter AO). The resulting wavelength-dependent point spread functions (PSFs) are characterized (see Figs 2-E to 14-E in AO) by an irregular oscillatory behaviour due to superposition of the diffraction patterns of primary and secondary mirrors, a total wavefront error of 0.05 wavelength RMS (at 633 nm), and an estimated pointing instability which causes image motion with 0.007 arcsec rms. As noted by Bendinelli *et al.* (1985), the oscillatory behaviour at longer wavelengths does not disappear after PSF integration over pixel surface and bandwidth, though it evidently becomes smoother. Also, because the pixel size is comparable with the separation of adjacent maxima, centring of HST images is critical for various problems such as, for instance, the detection of a faint star imbedded in the outer rings of a brighter one, or the determination of the dimensions of a nearby galaxy nucleus. For these reasons the attainment of a specific research objective by HST requires an 'ad hoc' data analysis, which must be improved on, awaiting for ST launch, by means of reliable simulations. Very comprehensive software packages for simulation of HST observations, taking into account of all known physical effects on images, are now available at the Space Telescope Science Institute (Burrows & Hasan 1986) and at the Space Telescope European Coordinating Facility (Rosa & Baade 1986). Nevertheless,

simulations can be performed more easily and in a less time-consuming way if simple analytical approximations of the PSF are available.

The purpose of this work is to provide a model of on-axis PSFs with circular symmetry, as in first approximation the WF/PC images could be, showing its usefulness by some examples of application to HST data analysis. Also, the search of a bidimensional approximation of the expected off-axis PSFs is in progress, based on the analysis of azimuthally asymmetric star images generated by the above simulation packages.

2. Monochromatic PSF approximation

2.1 *Long-wavelength PSFs*

The multimodal behaviour of the monochromatic PSFs of the space telescope at long wavelength suggests that their radial profiles $f(r)$ may be approximated by a mixture of N off-centred Gaussian functions, *i.e.*,

$$f(r)=(a_1/2\pi\sigma_1^2)\exp(-r^2/2\sigma_1^2)+\sum_{i=2}^{N} a_i k_i \exp[-(r-b_i)^2/2\sigma_i^2]. \quad (1)$$

In this equation a_i $\left(\text{with } \sum_{i=1}^{N} a_i = 1\right)$ is the repartition coefficient of the ith Gaussian, σ_i its dispersion parameter, b_i its distance from the centre of the whole image (note $b_1 = 0$) and k_i the normalization factor explicitly expressed by

$$k_i=[2\pi\sigma_i^2\exp(-b_i^2/2\sigma_i^2)+\pi^{3/2}\sqrt{2}\sigma_i b_i \operatorname{erfc}(-b_i/\sigma_i\sqrt{2})]^{-1}. \quad (2)$$

The capability of Equation (1) to give a very good approximation of the space telescope monochromatic PSFs is shown in Fig. 1, where the PSF at 552 nm is considered. It is evident that small differences are present only in the minima.

The $3N$–2 parameters involved in Equation (1) are obtained by means of the Newton-Gauss Regularized method (see Bendinelli *et al.* 1988, hereafter BA) which, in the present case, is very easy to apply. In fact, the contribution of the ith Gaussian becomes negligible outside the radial range $b_i \pm 3\sigma_i$ so that, breaking down the data, the parameters of a limited number of Gaussians must be estimated at any one time. The values of the parameters, obtained for a set of chosen wavelengths, are reported in Table 1.

The well-defined trend of parameter values at long wavelengths must be noted. It enables us to derive approximately the PSF at intermediate wavelengths by Interpolation.

Though monochromatic PSFs may be used for the simulation of some HST observations (and also for data reduction if the mechanical stress at the launch does not cause defocusing and misalignment), the majority of observations will be performed by wide-band filter. To define the mean PSF of a particular, wide-band image, the monochromatic PSFs must be weighted (see Westphal 1982; Macchetto 1982), accounting for the spectral type of the source, filter transmission, quantum efficiency of the telescope and light detector, as was done in the accurate work of Rosa & Baade (1986). This means that, rigorously, there is a PSF for any HST observation proposed,

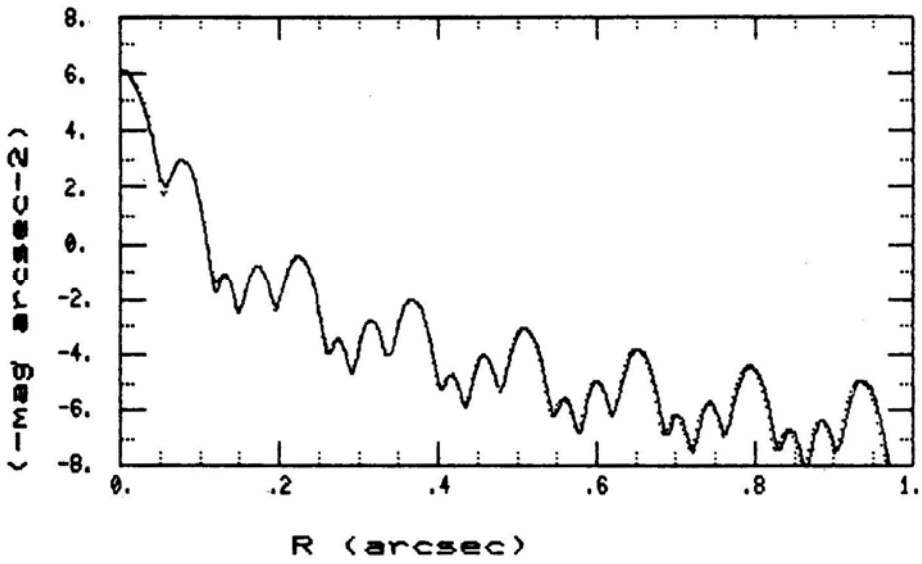

Figure 1. Comparison of the PSF at 552.5 nm (solid line) and its fit by off-centred Gaussians (dots).

and the more delicate the problem tackled the better must the PSF be known. Fortunately, the total weighting effect results in a general smoothing (increased by pixel integration), so that wide-band PSFs can be approximated by a reduced number of Gaussians. This happens since the smallest diffraction features are smeared out, as is shown in Fig. 2, where a rough weighted mean of the PSF in the *V* band is fitted with the parameters reported in Table 2.

2.2 *Short-wavelength PSFs*

It is known that at short wavelengths the effects of wavefront error and image motion are larger than the features of diffraction patterns, so that the expected monochromatic PSFs could be better described by smooth functions such as those proposed by Moffat (1959) and King (1983). But as is shown in BA, any smooth monotonically decreasing distribution can be fitted very well by a mixture of centred Gaussians, so that centring and convolution-deconvolution of nearly circular HST images does not present difficulties.

3. Two applications

In this section, two of the many problems concerning the analysis of HST data are briefly discussed based on the present monochromatic PSF approximation. Obviously they can be approached in the same way (and with less trouble) if wide-band observations and the Gaussian fit of their PSF are available.

Table 1. Computed coefficients for four monochromatic wavelengths.

	552.5 nm				656.3 nm			
	K	*a*	*σ*	*b*	*K*	*a*	*σ*	*b*
1	408.00	0.670E+00	0.185E−01	0.000	297.40	0.672E+00	0.216E−01	0.000
2	62.61	0.250E+00	0.130E−01	0.078	46.22	0.250E+00	0.148E−01	0.093
3	59.19	0.595E−02	0.811E−02	0.132	44.26	0.621E−02	0.916E−02	0.157
4	32.53	0.149E−01	0.113E−01	0.172	245.30	0.149E−02	0.126E−02	0.205
5	21.01	0.318E−01	0.135E−01	0.224	15.53	0.320E−01	0.153E−01	0.267
6	27.11	0.151E−02	0.851E−02	0.275	20.69	0.155E−02	0.939E−02	0.327
7	18.27	0.431E−02	0.110E−01	0.316	13.69	0.437E−02	0.124E−01	0.375
8	12.82	0.123E−01	0.135E−01	0.368	9.48	0.124E−01	0.153E−01	0.437
9	17.37	0.739E−03	0.874E−02	0.418	13.29	0.743E−03	0.963E−02	0.496
10	12.80	0.193E−02	0.108E−01	0.459	9.62	0.196E−02	0.121E−01	0.545
11	9.22	0.661E−02	0.135E−01	0.510	6.81	0.670E−02	0.154E−01	0.606
12	12.67	0.469E−03	0.894E−02	0.561	9.66	0.483E−03	0.987E−02	0.666
13	9.94	0.104E−02	0.106E−01	0.601	7.49	0.106E−02	0.119E−01	0.714
14	7.20	0.418E−02	0.135E−01	0.653	5.32	0.425E−02	0.154E−01	0.776
15	9.87	0.342E−03	0.915E−02	0.703	7.52	0.352E−03	0.101E−01	0.835
16	8.19	0.626E−03	0.104E−01	0.744	6.18	0.640E−03	0.116E−01	0.884
17	5.90	0.290E−02	0.135E−01	0.795	4.35	0.296E−02	0.155E−01	0.945
18	8.05	0.272E−02	0.933E−02	0.846				
19	6.99	0.404E−03	0.102E−01	0.886				
20	5.01	0.214E−02	0.135E−01	0.938				

	680.0 nm				815.0 nm			
	K	*a*	*σ*	*b*	*K*	*a*	*σ*	*b*
1	278.20	0.672E+00	0.223E−01	0.00	197.50	0.674E+00	0.263E−01	0.000
2	43.36	0.251E+00	0.153E−01	0.096	31.01	0.252E+00	0.178E−01	0.115
3	41.84	0.623E−02	0.936E−02	0.162	30.76	0.638E−02	0.106E−01	0.194
4	22.97	0.150E−01	0.130E−01	0.213	16.78	0.151E−01	0.149E−01	0.255
5	14.57	0.321E−01	0.158E−01	0.276	10.46	0.324E−01	0.183E−01	0.331
6	19.52	0.156E−02	0.961E−02	0.338	14.38	0.160E−02	0.109E−01	0.405
7	12.90	0.437E−02	0.127E−01	0.389	9.36	0.444E−02	0.146E−01	0.466
8	8.88	0.125E−01	0.158E−01	0.453	6.37	0.126E−01	0.184E−01	0.542
9	1.25	0.763E−02	0.985E−01	0.514	9.22	0.784E−03	0.112E−01	0.616
10	9.06	0.196E−02	0.124E−01	0.564	6.58	0.200E−02	0.143E−01	0.677
11	6.39	0.672E−02	0.158E−01	0.628	4.58	0.685E−02	0.184E−01	0.753
12	9.11	0.485E−03	0.101E−01	0.690	6.82	0.494E−03	0.113E−01	0.827
13	7.04	0.107E−02	0.122E−01	0.740	4.74	0.115E−02	0.151E−01	0.888
14	4.99	0.426E−02	0.158E−01	0.804				
15	7.23	0.350E−03	0.101E−01	0.865				
16	5.34	0.685E−03	0.130E−01	0.916				

3.1 *Centring of a star image*

An HST star image contains a large fraction of the total luminosity within the first minimum of diffraction pattern, hence its off-centring with respect to the central pixel (that of local maximum intensity) can be determined by the method proposed in BA (see also Chiu 1980), taking $N = 1$, *i.e.,* considering only the light distribution in the

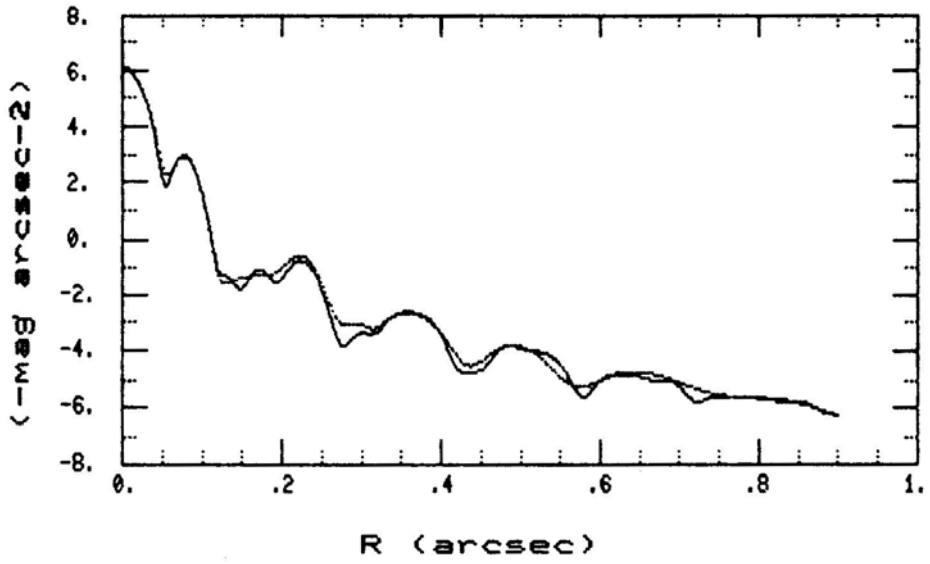

Figure 2. Comparison of the *V*-band PSF (solid line) and its fit (dots).

Table 2. Computed coefficients for *V*-band.

	K	*a*	*σ*	*b*
1	410.90	0.669E+00	0.186E−01	0.000
2	60.92	0.248E+00	0.135E−01	0.077
3	7.01	0.425E−01	0.538E−01	0.168
4	16.77	0.248E−01	0.169E−01	0.224
5	16.84	0.172E−02	0.128E−01	0.294
6	5.33	0.167E−01	0.332E−01	0.359
7	3.52	0.828E−02	0.367E−01	0.491
8	1.91	0.580E−02	0.520E−01	0.639
9	0.81	0.680E−02	0.994E−01	0.793

Airy disc. It must be stressed that the presence of b_i terms in Equation (1) prevents (as far as we know) expressing the complete marginal distributions by an analytical function, so that the BA method cannot be used to derive off-centring and all PSF parameters from the whole star image at the same time. In other words, the centring algorithm developed in BA for analysis of ground-based CCD star images is not applicable to HST frames to test if the wings of the in-orbit PSF are like their predictions. Nevertheless, at least in principle since handling of real noisy data may be considerably more difficult, the complete description of an HST star image—*i.e.* simultaneous estimate of off-centring, PSF parameters and background—can be derived considering the pixel-to-pixel intensity distribution along two orthogonal diameters crossing at the central pixel of the image.

If $2l$ is the pixel size and x_c, y_c (both $\leqslant l$) the offset of the centre of the star image with respect to the central pixel (x_p, y_p), the intensity level $i(x_n, y_m)$ of a pixel centred at (x_n,y_m) is given by

$$i(x_n, y_m) = L_T \sum_{i=1}^{N} a_i k_i \int_{x_0}^{x_F} \int_{y_0}^{y_F} \exp[-(\sqrt{x'^2 + y'^2} - b_i)^2/2\sigma_i^2]\,dx'dy' + f(x_n, y_m), \quad (3)$$

where

$$x_0 = x_n - l - x_c, \qquad y_0 = y_m - l - y_c,$$
$$x_F = x_n + l - x_c, \qquad y_F = y_m + l - y_c,$$
$$L_T = \sum_{nm} i(x_n, y_m) \qquad (n = 1,2, \ldots, M;\ m = 1, 2, \ldots, M),$$

and finally $f(x_n, y_m)$ is the background distribution.

We consider now the partial pixel sums along the x-diameter, which result in

$$S_x(x_n) = \sum_{r=1}^{n} i(x_r, y_p). \quad (4)$$

These sums can be rigorously expressed by means of an integral equation like Equation (3), with suitable integration limits, or in an approximate way, taking into account the reduced range of variability of y', by

$$S_x(x_n) \simeq L_T \sum_{i=1}^{N} a_i k_i \int_{-\infty}^{x_F} \exp[-(x' - b_i)^2/2\sigma_i^2]\,dx' + f(x_n - x_1) \quad (5)$$

$$= \Sigma_i A_i \{1 + \mathrm{erf}[(x_F - b_i)/\sqrt{2}\sigma_i]\} + f(x_n - x_1), \quad (6)$$

with $A_i = (2\pi)^{1/2}/lL_T\sigma_i a_i k_i$.

Since Equation (6) is differentiable with respect to the parameters x_c, A_i, σ_i, b_i and those of the background model, these can be derived by the Newton–Gauss regularized method (see BA for details).

Evidently, also $S_y(y_m)$, the sums along the y-axis, can be treated like $S_x(x_n)$, so that by comparison of analogous parameters it can be inferred if the in-orbit PSF is like the expected one.

3.2 *Convolution-deconvolution of small objects*

Convolution effects cannot be disregarded in the analysis of HST images of objects of small angular dimensions such as globular clusters in external galaxies, nuclei of nearby galaxies, overall profiles of normal and active galaxies at cosmological distances, and so on.

Dealing with non-undersampled objects, *i.e.,* those in which the searched features are not much smaller than pixel size, it can be easily derived that their apparent brightness profile $f(r)$ is related to the true radially symmetric profile $F(r)$ (including cosmological effects, if required) by the integral equation

$$f(r) = \sum_{i=1}^{N} 2a_i k_i \int_0^{\infty} sF(s)\Phi(r, s, \sigma_i, b_i)\,ds, \quad (7)$$

where, using the Gaussian mixture approximation of the PSF,

$$\Phi(r, s, \sigma_i, b_i) = \int_0^{\pi} \exp[-(s^2 + r^2 - 2rs\cos\theta + b_i^2 - 2b_i\sqrt{s^2 + r^2 - 2rs\cos\theta})/2\sigma_i^2]\,\mathrm{d}\theta \tag{8}$$

is evaluated by numerical integration. (For a remark on the analysis of undersampled data, see Section 4.2.)

Evidently Equation (7) can be used either to provide a set of convolved models of globular clusters or galaxies, as seen by HST, or for deconvolution (see Bendinelli, Parmeggiani & Zavatti 1986) of HST observations of the same objects.

In this case the resolution given by the pixel size may be insufficient, being comparable to the $\sigma\, i$; but a subpixel resolution is attainable by a set of frames, slightly shifted by a pixel fraction, obtained by exploiting the HST astrometric potential (see for instance Jefferys *et al.* 1985). Another possibility consists in determining *a posteriori* the relative displacements of the extended object with respect to the central pixels in a set of frames, by means of the off-centring of some stars around the object. It is worth noting that this procedure does not require the parallel use of one of the fine guidance sensors (FGS), and further that algebraic deconvolution works well even if the data are unequally spaced.

4. Concluding remarks

The usefulness of the present approximation of on-axis PSFs should have been sufficiently demonstrated by the examples of application shown, if the expected image quality will be kept in orbit. Nevertheless, some points deserve further comments.

4.1 *The wide-band PSFs*

In view of the importance of wide-band observations by the WF/PC camera in all astrophysical fields (see for instance 'The GTO observing program', STScI, October 1985) the parameters of the PSF multi-Gaussian model must be accurately re-calculated and the model compared with expected PSFs generated by the ST/ECF simulation code. This will be done in a future paper.

4.2 *HST resolution for extragalactic research*

Basically, the pixel size will give the resolution of a single HST observation, but if a set of images of the same object are obtained in conjunction with one of the FGS, or subjected to an astrometric analysis as outlined in Section 3.2), the resulting resolution would be a fraction of a pixel. Deconvolution of features of these dimensions seems therefore possible, improving the HST resolution. Further, a realistic PSF model can be of aid in reaching reliable inferences on the structure of a unresolved source (such as the nucleus of an external galaxy or the whole profile of a very distant one). A set of source models, in effect, can be easily convolved with PSF, integrated on pixel surface and compared with real undersampled data to select the most probable model.

Acknowledgements

We wish to thank G. G. C. Palumbo for careful reading of the manuscript and helpful comments, G. S. Djorgovski and an anonymous referee for their constructive criticism which has much improved the presentation of the paper, D. Iorio-Fili and P. Benvenuti for providing the ST/ECF simulation code. The Italian Piano Spaziale Nazionale is acknowledged for partial financial support (Contract PSN-85-078).

References

Bendinelli, O., Di Iorio, A., Parmeggiani, G., Zavatti, F.1985, *Astr. Astrophys*., **153,** 265.

Bendinelli, O.,Parmeggiani, G., Piccioni, A.,Zavatti, F.1988, *Astr. J.,* in press (BA).

Bendinelli, O., Parmeggiani, G., Zavatti, F. 1986, *Astrophys. J.,* **308,** 611.

Burrows, C, Hasan, H. 1986, preprint.

Chiu, L. T. G., 1980, *Celestial Mechanics,* **22,** 191.

Jefferys, W. H., Benedict, G. F., Hemenway, P. D., Shelus, P. J., Duncombe, R. L. 1985, *Celestial Mechanics,* **37,** 299.

King, I R. 1983, *Publ. astr. Soc. Pac,* **95,** 163.

Macchetto, F. 1982, in *The Space Telescope Observatory,* Ed. D. N. B. Hall, STScI, Baltimore, p. 40.

Moffat, A. F. J. 1969, *Astr. Astrophys.,* **3,** 455.

Rosa, M., Baade, D.1986, *The Messenger,* **45,** 22.

Westphal, J. A.1982, in *The Space Telescope Observatory,* Ed. D. N. B. Hall, STScI, Baltimore, p. 28.